Article

Cell Reports

Embryonic Microglia Derive from Primitive Macrophages and Are Replaced by *cmyb*-Dependent Definitive Microglia in Zebrafish

Graphical Abstract

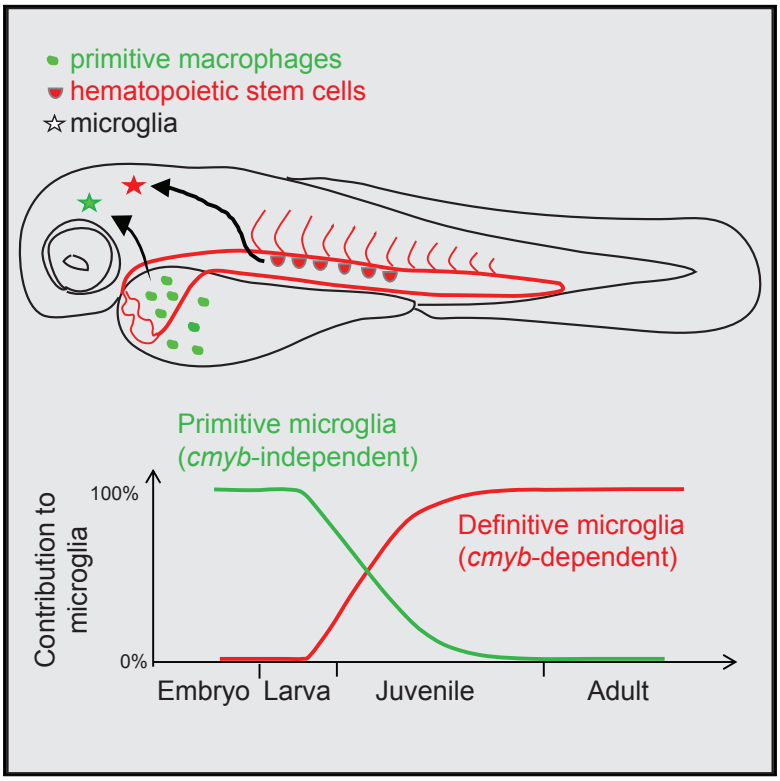

Highlights

- Microglia ontogeny occurs in two distinct waves in zebrafish
- EMPs do not contribute to microglia development
- Primitive macrophages give rise to primitive microglia
- Embryonic HSCs give rise to adult definitive microglia

Authors

Giuliano Ferrero, Christopher B. Mahony, Eléonore Dupuis, ..., David Traver, Julien Y. Bertrand, Valérie Wittamer

Correspondence

dtraver@ucsd.edu (D.T.), julien.bertrand@unige.ch (J.Y.B.), vwittame@ulb.ac.be (V.W.)

In Brief

Using zebrafish to investigate microglia ontogeny during vertebrate development, Ferrero et al. find that embryonic "primitive" microglia exclusively derive from primitive macrophages, while adult "definitive" microglia originate from *cmyb*-dependent hematopoietic stem cells.

Ferrero et al., 2018, Cell Reports *24*, 130–141
July 3, 2018
https://doi.org/10.1016/j.celrep.2018.05.066

CellPress

OPEN ACCESS
CellPress

Cell Reports
Article

Embryonic Microglia Derive from Primitive Macrophages and Are Replaced by *cmyb*-Dependent Definitive Microglia in Zebrafish

Giuliano Ferrero,[1,2,3] Christopher B. Mahony,[4] Eléonore Dupuis,[1] Laurent Yvernogeau,[5] Elodie Di Ruggiero,[1,2] Magali Miserocchi,[1] Marianne Caron,[1,2,3] Catherine Robin,[5,8] David Traver,[6,7,9,*] Julien Y. Bertrand,[4,9,*] and Valérie Wittamer[1,2,3,9,10,*]

[1]Institut de Recherche Interdisciplinaire en Biologie Humaine et Moléculaire (IRIBHM), Université Libre de Bruxelles (ULB), Brussels, Belgium
[2]ULB Institute of Neuroscience (UNI), ULB, Brussels, Belgium
[3]WELBIO, ULB, Brussels, Belgium
[4]Department of Pathology and Immunology, University of Geneva, School of Medicine, Geneva, Switzerland
[5]Hubrecht Institute-KNAW and University Medical Center, Utrecht, the Netherlands
[6]Department of Cellular and Molecular Medicine, University of California, San Diego, 9500 Gilman Drive, La Jolla, CA 92093-0380, USA
[7]Section of Cell and Developmental Biology, University of California, San Diego, 9500 Gilman Drive, La Jolla, CA 92093-0380, USA
[8]Regenerative Medicine Center, University Medical Center, Utrecht, the Netherlands
[9]These authors contributed equally
[10]Lead Contact
*Correspondence: dtraver@ucsd.edu (D.T.), julien.bertrand@unige.ch (J.Y.B.), vwittame@ulb.ac.be (V.W.)
https://doi.org/10.1016/j.celrep.2018.05.066

SUMMARY

Microglia, the tissue-resident macrophages of the CNS, represent major targets for therapeutic intervention in a wide variety of neurological disorders. Efficient reprogramming protocols to generate microglia-like cells *in vitro* using patient-derived induced pluripotent stem cells will, however, require a precise understanding of the cellular and molecular events that instruct microglial cell fates. This remains a challenge since the developmental origin of microglia during embryogenesis is controversial. Here, using genetic tracing in zebrafish, we uncover primitive macrophages as the unique source of embryonic microglia. We also demonstrate that this initial population is transient, with primitive microglia later replaced by definitive microglia that persist throughout adulthood. The adult wave originates from *cmyb*-dependent hematopoietic stem cells. Collectively, our work challenges the prevailing model establishing erythro-myeloid progenitors as the sole and direct microglial precursor and provides further support for the existence of multiple waves of microglia, which originate from distinct hematopoietic precursors.

INTRODUCTION

Microglia (MG) represent a distinct population of mononuclear phagocytes that serve multiple functions in central nervous system (CNS) physiology and disease (Colonna and Butovsky, 2017; Wolf et al., 2017). They are distributed throughout the brain and spinal cord parenchyma, accounting for up to 15% of total glial cells. As resident phagocytes in the CNS, MG act as immune sentinels and constitute the first line of defense in response to local infection or injury. Elegant live-imaging studies in mouse (Davalos et al., 2005; Nimmerjahn et al., 2005) and zebrafish (Li et al., 2012; Peri and Nüsslein-Volhard, 2008; Sieger et al., 2012) have shown that MG constantly survey their surroundings through highly motile cellular processes and quickly react to pathological stimuli by adopting morphological changes and stimulus-dependent phenotypes (Ransohoff and Cardona, 2010). In addition to their role as immune effectors, MG also perform numerous key functions in the development and homeostasis of the CNS, including removal of cellular debris from apoptotic neurons, production of trophic factors, synaptogenesis, and injury repair. While it was generally believed that MG do not contribute directly to CNS pathologies, increasing evidence now indicates that defective MG can be directly causative in several neurological disorders (Guerreiro et al., 2013; Mass et al., 2017; Paloneva et al., 2002; Rademakers et al., 2011). These observations have increased the general interest in targeting MG for therapeutic purposes. Understanding the precise developmental program of MG has thus become a major goal of the field, as it will advance current reprogramming protocols for generation of MG-like cells *in vitro* for therapeutic use or to model disease in a dish.

Previous findings in humans (Boche et al., 2013), mice (Alliot et al., 1999), chicken (Cuadros et al., 1993), and zebrafish (Herbomel et al., 1999) have demonstrated that MG are established early during embryogenesis. Additional studies using parabiotic mice have revealed that adult MG in the steady state are autonomously maintained in the CNS through proliferation, with no contribution of bone marrow-derived progenitor cells (Ajami et al., 2007; Mildner et al., 2007). Across the vertebrate phylum, myelopoiesis occurs in three distinct waves (Bertrand et al., 2005). In mice, the two first waves originate in the yolk sac and give rise to primitive macrophages (pMFs) and erythro-myeloid progenitors (EMPs) at embryonic day 7.5 (E7.5) and E8.25,

respectively. A third wave of macrophages (MFs) is produced by hematopoietic stem cells (HSCs) after they emerge at E10.5 within the embryo proper (Medvinsky et al., 2011). Using newly generated lineage-tracing tools in the mouse model, several groups have attempted to identify the cellular origin of MG, with conflicting conclusions. Using a *Runx1*:MER-CRE-MER knockin allele, Ginhoux et al. (2010) concluded that adult MG derive from pMFs during murine embryogenesis. More recent studies identified the EMP as the sole and direct precursor of embryonic and perinatal mouse MG (Gomez Perdiguero et al., 2015; Kierdorf et al., 2013). These discordant results highlight the difficulty of performing in utero selective labeling of specific hematopoietic populations that all arise within a very narrow temporal window during development. Moreover, as yolk sac-derived hematopoietic precursors share multiple markers and temporally overlap, the relative contribution of each cell subset to MG ontogeny cannot be faithfully addressed using the inducible fate-mapping models currently available in the mouse (reviewed in McGrath et al., 2015). Also, in these fate-mapping experiments, only a subset of MG found in adult mice were genetically labeled, leaving open the possibility of the existence of multiple sources of MG progenitors during vertebrate development. Interestingly, a previous study in the zebrafish using controlled temporal and spatial lineage tracing suggested that two waves originating from distinct anatomical locations are responsible for the establishment of the MG network (Xu et al., 2015). This work, however, did not identify the precise nature of the hematopoietic progenitors involved in MG formation. In conclusion, the prevailing view that EMPs serve as the unique and direct precursor of MG may need reassessment, using better tools to precisely label each possible progenitor subset. Here, we utilized the unique strengths of the zebrafish model, where each possible precursor of MG (pMFs, EMPs, and HSCs) is spatially and temporally distinct during embryonic development, to refine our understanding of MG ontogeny in the vertebrate embryo.

RESULTS

Zebrafish MG Display Similar Features to Their Mammalian Counterparts

We initially investigated the MF populations present in the brain of adult zebrafish, using two transgenic lines where the class II major histocompatibility beta chain (*mhc2dab*) and the *cd45* promoters drive GFP and DsRed, respectively. As we previously described, co-expression of these fluorescent transgenes specifically labels cells of the mononuclear phagocyte system in zebrafish (Wittamer et al., 2011). Confocal microscopy of adult brain sections from Tg(*cd45:DsRed;mhc2dab:GFP*) double-transgenic animals demonstrated a dense network of double-positive cells that displayed the typical ramified MG morphology (Figure 1A). By flow cytometry, two cell populations could be discriminated in the brain based on *cd45:DsRed* expression (Figure 1B). qPCR analyses indicated that *cd45*^{low}*mhc2*$^{+}$ cells expressed high levels of the MG-specific genes apolipoprotein Eb (*apoeb*) and purinergic receptor p2y12 (*p2ry12*) (Butovsky et al., 2014), and low levels of macrophage-expressed gene 1 (*mpeg1*), a MF-specific marker (Ellett et al., 2011) (Figure 1C). In contrast, *mpeg1* was abundantly expressed in *cd45*^{high}*mhc2*$^{+}$ cells, whereas MG-specific transcripts were nearly undetectable (Figure 1C). Other markers, previously shown to be expressed in murine MG (Butovsky et al., 2014), such as *C1qc*, *csf1ra*, and *csf3r,* were also highly enriched in *cd45*^{low}*mhc2*$^{+}$ cells when compared to *cd45*^{high}*mhc2*$^{+}$ cells (Figure 1C). Thus, the *cd45*^{low} population represents parenchymal MG, whereas *cd45*^{high} cells likely represent non-parenchymal CNS-associated MFs, consistent with the use of *CD45* for their discrimination in mammals (Schmid et al., 2009). Based on the differential expression of *mpeg1* transcripts between *cd45*^{high} and *cd45*^{low} populations, we further showed that fluorescence expression in the MF *mpeg1:GFP* transgenic reporter (Ellett et al., 2011) enabled similar MG purification and histological detection from adult zebrafish (Figures 1D–1F). Collectively, these findings demonstrate that MG identity has been conserved through evolution and provide reliable techniques for their prospective isolation from the adult brain.

Embryonic MG Do Not Originate from Definitive Hematopoietic Precursors

MG development in the zebrafish embryo occurs around 60 hr post-fertilization (hpf) (Herbomel et al., 2001), when the differentiation marker *apoeb* becomes first detectable in *mpeg1:GFP*$^{+}$ cells (Figure 1G). To investigate the identity of embryonic MG precursors, we first examined the expression of *apoeb* in mutants with defective embryonic hematopoiesis. One potential precursor population is HSCs, which derive from the hemogenic endothelium of the aorta between 36 and 54 hpf (Bertrand et al., 2010; Kissa and Herbomel, 2010). Analysis of *cmyb* mutant embryos, which completely lack HSCs (Soza-Ried et al., 2010), revealed no difference in the number of *apoeb*$^{+}$ cells at 4 days post-fertilization (dpf) (Figures 2A and 2A′). This observation demonstrates that the hematopoietic precursors that seed the developing brain to generate embryonic MG do not derive from HSCs, consistent with previous findings in mice (Schulz et al., 2012) and zebrafish (Xu et al., 2015). We next investigated the possibility that EMPs might be responsible for generating MG. We previously identified EMPs, oligopotent progenitors endowed with erythroid and myeloid potential that arise from the posterior blood island (PBI), in zebrafish (Bertrand et al., 2007). Zebrafish EMPs express low levels of *cd41*, similar to yolk sac-derived murine EMPs (Frame et al., 2013). They are present in the embryo between 30 and 48 hpf, and can be isolated by flow cytometry from Tg(*lmo2:GFP; gata1:DsRed*) double-transgenic animals based on their *lmo2*^{high}*gata1*$^{+}$ phenotype (Bertrand et al., 2007). Recently, we identified the transcription factor *tfec* (*P2* isoform) as a regulator of the HSC niche (Mahony et al., 2016). Whereas *tfec-P2* was specifically expressed in the vascular niche, the *tfec-P3* variant was highly enriched in EMPs (Figure S1A). We therefore reasoned that *tfec* might also be important for EMP biology and that EMP specification or function might be perturbed following modulation of *tfec* activity. Whereas the disruption of *tfec*-mediated transcriptional activity had no effect on EMP specification (by overexpressing mRNA coding for the dominant-negative *tfec*) (Mahony et al., 2016) (Figures S1B–S1D′), the expression of key myeloid genes was strongly decreased in purified EMPs (Figure S1E), resulting in

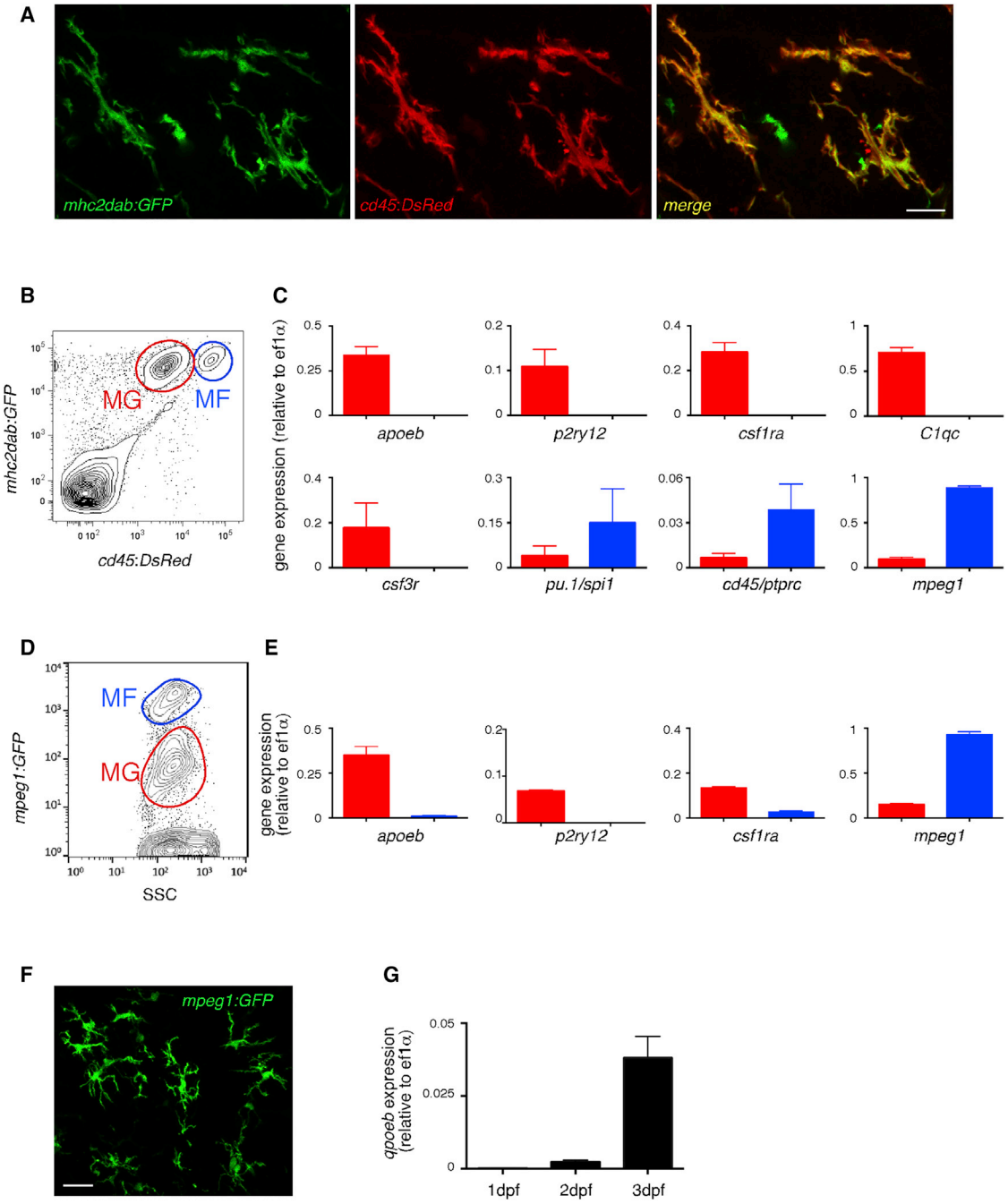

Figure 1. MG Identity Is Conserved in the Zebrafish

(A) Fluorescence of GFP (left panel) and DsRed (middle panel) in the brain of adult *cd45:DsRed; mhc2dab:GFP* double-transgenic fish. The right panel shows a merge of both fluorescent channels (n = 3). Scale bar: 10 μm.

(B) Flow cytometry analysis on brain cell suspensions from adult Tg(*cd45:DsRed; mhc2dab:GFP*) identifying *cd45*:DsRed^{low}*mhc2dab:GFP*$^{+}$ MG (red gate, MG) and *cd45:*DsRed^{high}*mhc2dab:GFP*$^{+}$ CNS-associated macrophages (blue gate, MFs).

(C) Comparison of the relative expression of *apoeb*, *p2ry12*, *csf1ra*, *C1qc*, *csf3r*, *mpeg1*, *pu.1/spi1b*, and *cd45/ptprc* transcripts between MG (red bars) and MFs (blue bars) cell subsets isolated by FACS. Error bars represent mean ± SD (n = 3).

(D and E) Flow cytometry of a brain cell suspension from adult *mpeg1:GFP* transgenics (D) and expression of *apoeb*, *p2ry12*, *csf1ra*, and *mpeg1* by qPCR in FACS-sorted *mpeg1:GFP*$^{+}$ cell subsets (E). Error bars represent mean ± SD (n = 3).

(F) GFP immunohistochemistry on adult *mpeg1:GFP* brain sections. Scale bar: 25 μm.

(G) *apoeb* expression in *mpeg1:GFP*$^{+}$ cells sorted at 1, 2, and 3 dpf. MG, microglia; MFs, macrophages.

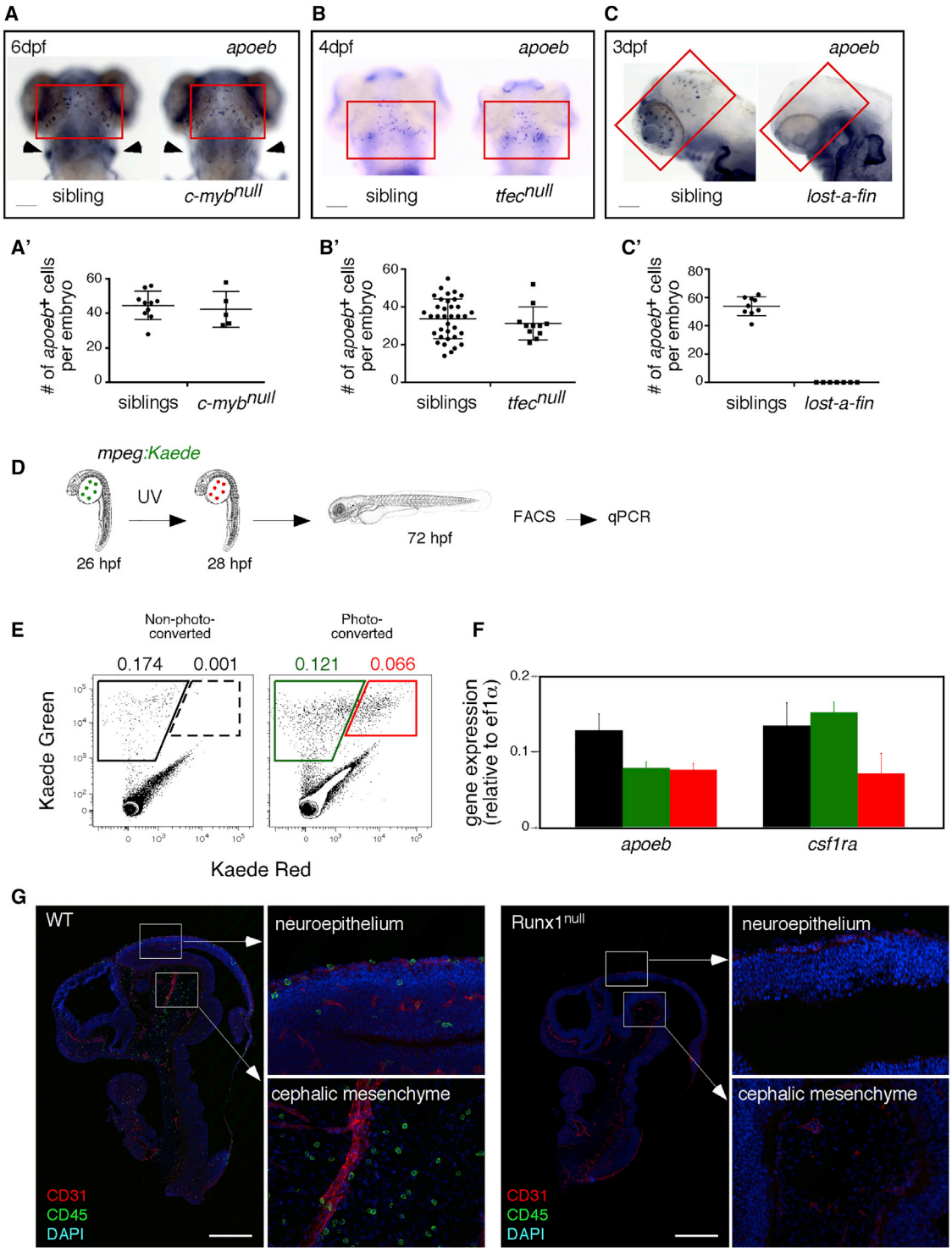

Figure 2. pMFs Are the Unique Source of MG in the Vertebrate Embryo

(A–C) Expression of the MG marker *apoeb* (red quadrants) in the brains of *cmyb*^{null} (A), *tfec*^{null} (B), *alk8*^{null} (*lost-a-fin*) (C), and their sibling control animals at the indicated developmental stages. For (A), *cmyb*^{null} embryos are identified by the concomitant absence of lymphoid-specific *rag1* (arrowheads) transcripts in the thymus. Scale bar: 50 μm.

(A′–C′) Quantification of *apoeb*$^{+}$ MG in embryos of indicated genotypes. Each symbol represents a single embryo. Error bars represent mean ± SEM.

(D) Strategy for transient fate mapping of pMFs *in vivo*.

(legend continued on next page)

decreased myelopoiesis in *tfec*-impaired animals at 48 hpf in the caudal hematopoietic tissue (CHT), the niche for EMP differentiation (Figure S1F). These observations indicate that EMPs show altered differentiation potential in response to *tfec* loss of function. However, MG numbers were similar between *tfec*^{null} embryos and their siblings at 4 dpf (Figures 2B and 2B′), strongly suggesting that EMPs are not responsible for establishing embryonic MG. Together, these results exclude definitive hematopoietic progenitors (EMPs and HSCs) as the origin of MG initially present in the zebrafish embryo.

pMFs Are the Unique Source of MG in the Vertebrate Embryo

Because primitive myelopoiesis develops normally in *cmyb*^{nul} (Soza-Ried et al., 2010) and *tfec*^{null} embryos (Figures S1G and S1G′), we reasoned that embryonic MG likely derived from pMFs. Indeed, we observed a complete absence of MG in *lost-a-fin* mutant embryos that lack primitive myelopoiesis (Hogan et al., 2006) (Figures 2C and 2C′). To trace directly the fate of pMFs, we examined animals carrying the *mpeg1:Kaede* transgene, which encodes a green-to-red photoconvertible fluorophore under control of the MF-specific *mpeg1* promoter (Ellett et al., 2011). *Kaede*$^{+}$ embryos were photoconverted between 26 and 28 hpf (a time when *kaede* is expressed only in pMFs), and their progeny was analyzed by flow cytometry at 72 hpf (Figures 2D and 2E). Photoconverted cells expressed the MG marker *apoeb* and the MF transcript *csf1ra* (Figures 2E and 2F), thus indicating that pMFs contribute to MG at 72 hpf. In agreement with a previous report (Xu et al., 2016), we also observed that colonization of the brain by pMFs did not require blood flow, since MG numbers were normal in 60 hpf *silent heart* mutants that lack blood circulation (Figure S2). These findings strengthen pMFs as the unique origin of embryonic MG in zebrafish since seeding of the developing brain by PBI-derived EMPs would likely depend upon circulation.

In the mouse, fate-mapping studies have led to the consensus that EMPs generate embryonic and perinatal MG (Prinz et al., 2017). One discrepancy, however, is that *c-Myb*$^{-/-}$ mouse embryos, which lack HSCs and display strongly impaired EMPs (based on phenotype and functional analyses) (Sumner et al., 2000), show normal embryonic MG numbers (Kierdorf et al., 2013; Schulz et al., 2012), therefore strongly pointing to *c-Myb*-independent pMFs (Schulz et al., 2012) as the precursors of murine embryonic MG. To reconcile these findings and investigate whether our observations in zebrafish were conserved across evolution, we analyzed *Runx1*$^{-/-}$ mouse embryos, which differ notably from *c-Myb*$^{-/-}$ embryos by the additional absence of pMFs (Figure S3; Table S1). Initial seeding of the mouse brain parenchyma by MG progenitors has been reported at around E10. We therefore evaluated the presence of CD45^{+} MG progenitors in E10.5 *Runx1*$^{-/-}$ embryos. In contrast to *c-Myb*$^{-/-}$ embryos, MG were completely absent in *Runx1*$^{-/-}$ embryos, correlating with the absence of pMFs (Figure 2G). These results suggest that, as observed in the zebrafish, embryonic MG in the mouse correlate with the presence of pMFs but not with definitive hematopoietic progenitors (EMPs and HSCs) (Table S1).

MG Ontogeny Proceeds into Two Distinct Waves

We returned to the zebrafish model to further investigate the fate of pMF-derived MG. Because the transient nature of the photoconverted *kaede* precluded long-term analyses, we turned to a Cre-lox system to enable indelible cell labeling. To overcome the lack of a specific marker for pMFs, we developed a strategy to distinguish primitive versus definitive hematopoietic waves based on their origin, and used the endothelial-specific constitutive *kdrl:Cre*, in combination with the lineage marker *actb2:loxP-STOP-loxP-DsRed* (also known as *ßactin:Switch-DsRed*). As we previously demonstrated, the *kdrl* promoter drives expression in hemogenic endothelium, resulting in HSCs and their progeny being permanently labeled in Tg(*kdrl:Cre*; *ßactin:Switch-DsRed*) double-transgenic animals (Bertrand et al., 2010). Since EMPs also arise from an endothelial precursor in mice (Chen et al., 2011; Frame et al., 2016), we hypothesized that, similar to their murine counterparts, zebrafish EMPs would also originate from hemogenic endothelium and would therefore be marked in the Tg(*kdrl:Cre; ßactin:Switch-DsRed*) combination. This strategy should thus label both definitive precursor populations but spare pMFs that originate directly from mesoderm (Herbomel et al., 1999). Supporting this postulate, fluorescent confocal microscopy analysis of Tg(*kdrl:*Cre*; ßactin:Switch-DsRed; cd41:eGFP*) triple-transgenic embryos revealed the presence of *cd41*^{lo}*DsRed*$^{+}$ EMPs within the vascular walls of the caudal hematopoietic tissue at 30 and 36 hpf (Figure S4A), thus demonstrating their endothelial origin in zebrafish. In contrast, when Tg(*kdrl:Cre; ßactin:Switch-DsRed*) were crossed to the MF-specific *mpeg1:GFP* reporter, we never observed GFP^{+} pMFs to express DsRed, at any time from their emergence in the rostral blood island to their migration over the yolk ball at 30 hpf (Figures 3B and S4B). A quantification of 119 GFP^{+} pMFs (from 14 embryos) demonstrated that 100% of this population was indeed DsRed^{-}. Importantly, in Tg(*kdrl:Cre; ßactin:Switch-DsRed; mpeg1:GFP*) embryos, the absence of DsRed expression in pMFs was not due to a delay in fluorophore synthesis, as these cells remained GFP^{+}DsRed^{-} over time, as observed by confocal microscopy later during development (Figure S4B). Therefore, in Tg(*kdrl:Cre; ßactin:Switch-DsRed; mpeg1:GFP*) embryos, the differential expression between DsRed^{-} pMFs

(E) Flow cytometry showing absence of *kaede-Red* expression in non-photoconverted embryos (left panel), whereas cells expressing both forms of *kaede* were present and sortable in the photoconverted embryos (right panel).
(F) qPCR analyses for *apoeb* and *csf1ra* on *mpeg1:kaede-Green* cells sorted from control and photoconverted embryos, and on *mpeg1:kaede-Green/Red* cells from photoconverted embryos. The color code matches the gates on the FACS plots. Error bars represent mean ± SD (n = 3 experiments).
(G) Sagittal sections of E10.5 *Runx1*^{null} embryos and their littermates (upper body) immunostained for CD31 (vascular) and CD45 (hematopoietic) markers, with DAPI used as a nuclear counterstain. Tile-scanned images show that *Runx1*^{null} mutants are completely devoid of CD45^{+} MG in the neuroepithelium and cephalic mesenchyme (n = 3). Scale bar: 500 μm.
See also Figures S1–S3.

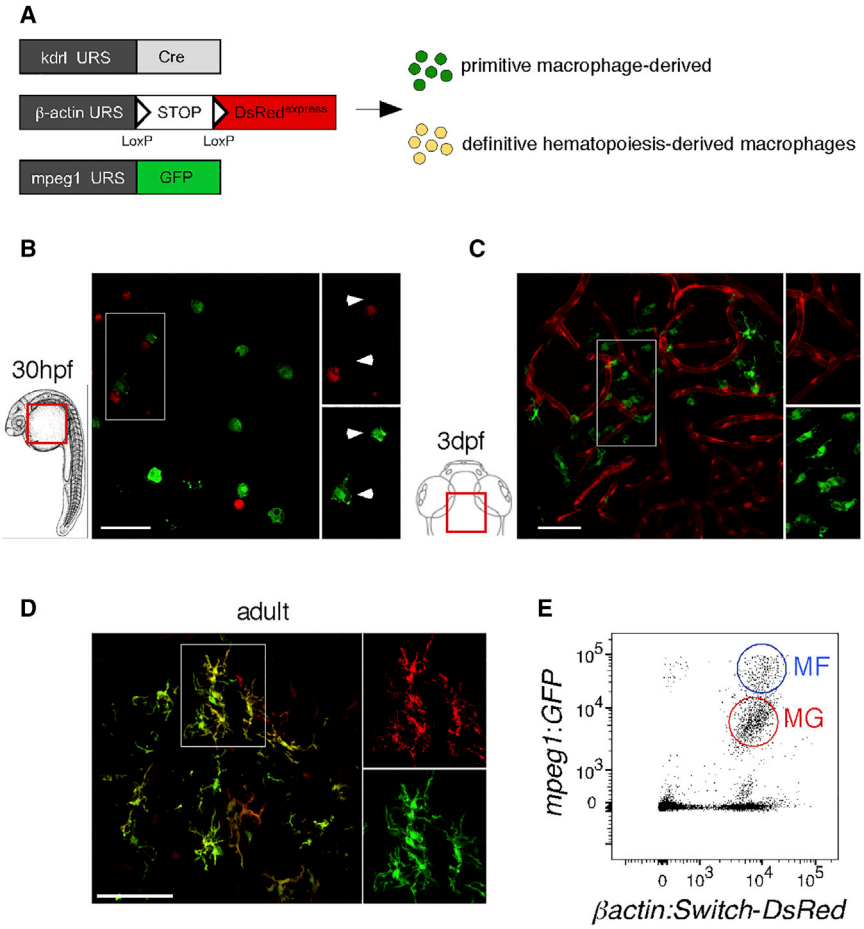

Figure 3. Embryonic and Adult MG Have Distinct Origins

(A) Scheme of the transgenic lines used to address the MG potential of primitive versus definitive hematopoiesis.

(B and C) Whole-mount fluorescence microscopy images of *Tg(kdrl:Cre; ßactin:Switch-DsRed; mpeg1:GFP)* triple-transgenic embryos show absence of DsRed expression (red) in GFP^+ pMFs (green) on the yolk ball at 30 hpf (B), and in GFP^+ embryonic MG (green) in the brain parenchyma at 3 dpf (C) (n = 14).

(D) In contrast, in sections of adult triple-transgenic animals, DsRed labeling is observed in all GFP^+ MG cells.

(E) Flow cytometry analysis on a brain dissected from a 12-week-old triple-transgenic animal identifies blood-derived *mpeg1:GFP*^{high} CNS-associated MFs (blue circle, MFs) and *mpeg1*:GFP^{low} MG (red circle, MG). Both populations express the *DsRed* reporter at high level (n = 5). Scale bar: 50 μm. MFs, macrophages; MG, microglia.

See also Figures S4 and S5.

versus $DsRed^+$ definitive hematopoietic precursors can be used to investigate their relative contribution to MG ontogeny (Figure 3A). Concordant with our initial observations, *mpeg1:GFP*$^+$ MG cells at 3 dpf were $DsRed^-$ (Figures 3B and 3C), thus validating a direct and exclusive lineage relationship with pMFs, further excluding EMPs as a precursor for embryonic MG.

Interestingly, when Tg(*kdrl:Cre; ßactin:Switch-DsRed; mpeg1:GFP*) zebrafish were raised to adulthood and subjected to further examination, we observed that *mpeg1:GFP*^{low} MG all expressed DsRed (Figure 3D). Fluorescence-activated cell sorting (FACS) analyses of brain cell suspensions confirmed that the entire *mpeg1:GFP*^{low} MG population was labeled by DsRed in adult transgenic animals (Figure 3E). Because the *kdrl* promoter activity is rapidly extinguished during the endothelial-to-hematopoietic transition (Bertrand et al., 2010) and is not detected in MG (Figure S5), this color switch indicates that embryonic and adult MG have distinct cellular origins in zebrafish, as previously suggested (Xu et al., 2015). Time course analyses of Tg(*kdrl:Cre; ßactin:Switch-DsRed; mpeg1:GFP*) larvae further demonstrated that colonization of the brain parenchyma by *DsRed*$^+$ MG initiates at around 2 weeks of age, leading to the complete replacement of embryonic *DsRed*$^-$ MG by 3 months (Figure 4). Therefore, our results demonstrate the existence of two successive waves of MG that can be discriminated based upon the hemogenic nature of their precursors. The first primitive wave originates from pMFs at 3 dpf, whereas the second wave gives rise to definitive adult MG, starting at around 20 dpf.

cmyb Requirement Discriminates Embryonic versus Adult MG

Since our fate-mapping results indicated that definitive MG derive from *kdrl*$^+$ hemogenic endothelium, we hypothesized that the second MG wave originated from definitive hematopoietic precursors and examined MG ontogeny in *cmyb*-deficient zebrafish that lack HSCs. To overcome the lethality due to the lack of HSCs and allow for long-term analyses, we rescued mutant embryos by hematopoietic cell transplantation, as previously described (Hess et al., 2013; Traver et al., 2003). Also, to allow for the rapid screening of recipient *cmyb*^{null} embryos and for the visualization of host-derived MG, we incrossed adult *cmyb* heterozygous fish carrying the following reporter transgenes: Tg(*kdrl:Cre*; *ßactin:Switch-DsRed*; *mpeg1:GFP*) (Figure 5A). *cmyb*^{null} embryos were identified at 5 dpf based on the absence of HSC-derived *DsRed*$^+$ thymocytes and selected for transplantation. Transplantation experiments were conducted using adult whole-kidney marrow (WKM) isolated from *cd41:GFP* transgenic adults, allowing for continued production of *GFP*$^+$ thrombocytes to serve as a readout for efficient long-term reconstitution. The mutually exclusive expression of both *cd41:GFP* and *mpeg1:GFP* transgenes, together with the typical cell shape of MG versus thrombocytes, prevented any possible issue regarding the discrimination between either GFP^+ population when analyzing the brain parenchyma. Rescued *cmyb*^{null} *kdrl:Cre*$^+$ *ßactin:Switch-DsRed*$^+$ *mpeg1:GFP*$^+$ embryos were then raised to adulthood (>3 months) before examination. By performing immunostaining on adult brain sections, we found a

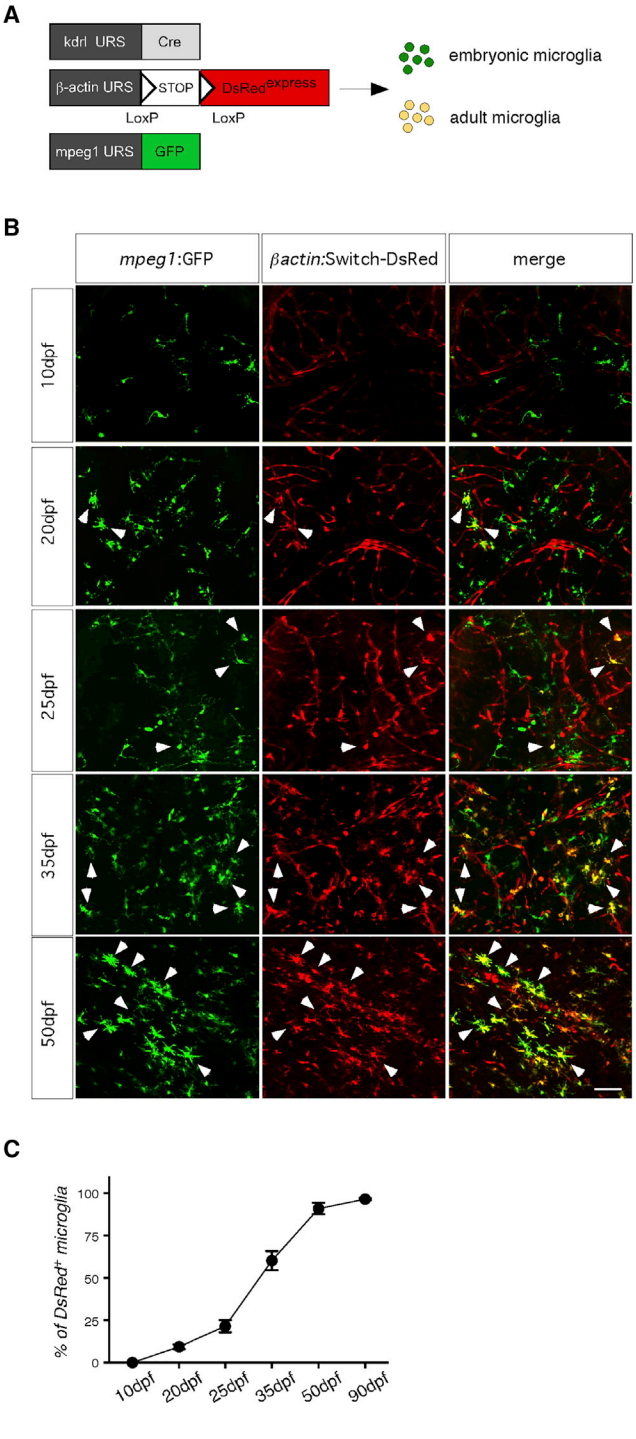

Figure 4. Kinetics of Adult MG Emergence during Zebrafish Development

(A) Scheme of the transgenic lines used to discriminate pMF-derived embryonic MG from endothelial-derived adult MG.

(B) GFP (left panels) and DsRed (middle panels) immunostaining performed on brain sections from Tg(*kdrl:Cre; ßactin:Switch-DsRed; mpeg1:GFP*) triple transgenics at the indicated developmental stage, showing the replacement of GFP$^+$ DsRed$^-$ embryonic MG by GFP$^+$ DsRed$^+$ cells in the brain parenchyma. The right panels show a merge of both fluorescent channels. Scale bar: 50 μm.

(C) Quantification of DsRed$^+$ MG in the brain parenchyma during zebrafish development, determined as percent recombination among the whole GFP$^+$ MG population. Error bars represent mean ± SEM of pooled data from two experiments (n = 3). MG, microglia.

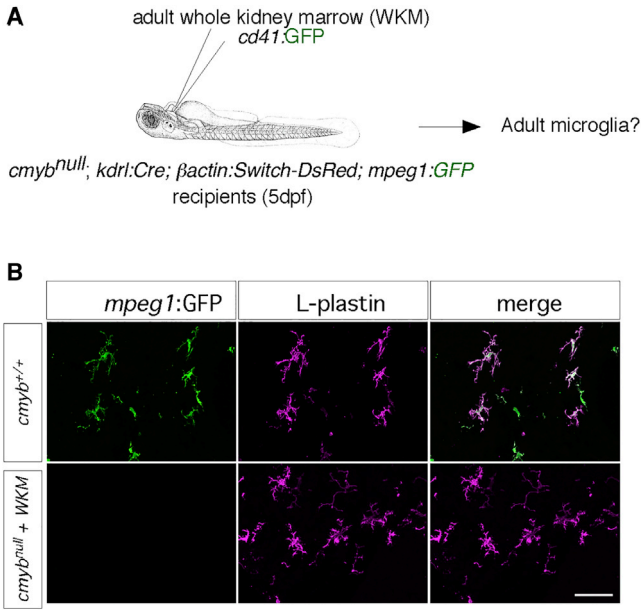

Figure 5. The Transcription Factor *cmyb* Is Required for the Establishment of Adult MG

(A) Scheme of the hematopoietic cell transplantation experiments performed to circumvent the lethality of *c-myb*^{null} animals due to the lack of definitive hematopoiesis.

(B) GFP immunostaining performed on adult brain sections from wild-type controls (upper panels) and rescued *cmyb*^{null} mutants (lower panels), demonstrating a complete absence of host-derived GFP$^+$ MG in the *cmyb* mutants (left panels), as well as the presence of GFP$^-$ donor-derived *L-plastin*$^+$ hematopoietic cells (fuchsia, middle panels). The right panels show a merge of both fluorescent channels (n = 4). Scale bar: 50 μm.

complete absence of host-derived GFP$^+$ MG in the rescued *cmyb*^{null} animals (n = 3) (Figure 5B). Interestingly, staining of *cmyb*^{null} adult brains with the pan-leukocyte L-plastin antibody revealed CNS engraftment of ramified L-plastin$^+$ GFP$^-$ cells, likely of donor origin (Figure 5B). Collectively, these observations demonstrate that *cmyb* is critical for the establishment and/or maintenance of adult MG precursors.

Embryonic HSCs Give Rise to Adult MG

Because endogenous MG were absent in adult *cmyb*^{null} fish that lack HSCs, we reasoned that HSCs may be the precursors of the second MG wave. As we previously showed, *gata2b* serves as an early marker of hemogenic endothelium in the dorsal aorta of the zebrafish embryo, and lineage tracing performed in Tg(*gata2b:Gal4; UAS:Cre*; *ßactin:Switch-DsRed*) reporter lines selectively and permanently labeled emerging HSCs and their adult blood progeny (Butko et al., 2015). To directly assess the contribution of HSCs to adult MG, we crossed Tg(*gata2b:Gal4; UAS:Cre*; *ßactin:Switch-DsRed*) transgenic animals to

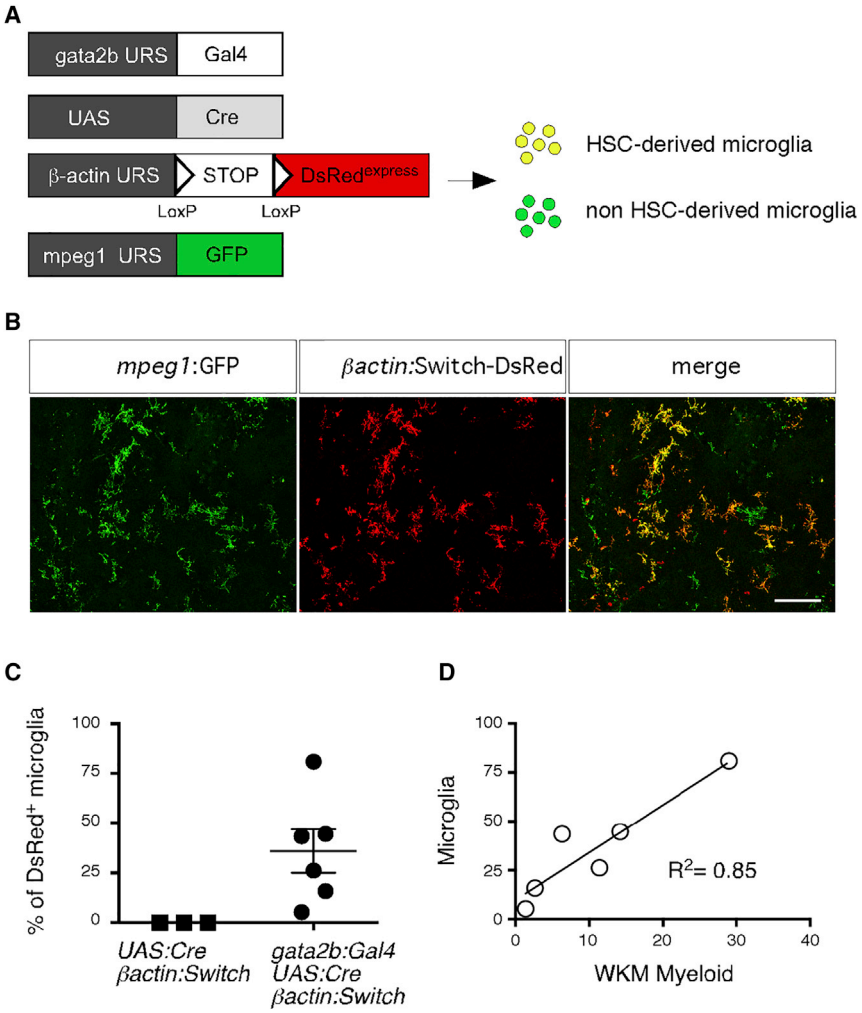

Figure 6. Adult MG Derive from Embryonic HSCs

(A) Transgenic lines used to address the MG potential of embryonic HSCs.

(B) GFP (left panel) and DsRed (middle panel) immunostaining performed on quadruple-transgenic adult brain sections. The right panel shows a merge of both fluorescent channels.

(C) Pooled data from two experiments showing the percent recombination among brain MG in control (left) and *gata2b:Cre* adult fish (right) (n = 6). Error bars represent mean ± SEM.

(D) Correlation and regression analysis (R^2 = 0.85) between the chimerism in brain MG and the WKM myeloid fraction. MG, microglia; WKM, whole-kidney marrow.

See also Figure S6.

the *mpeg1:GFP* reporter line (Figure 6A). As expected, in 3 dpf quadruple-transgenic embryos, DsRed fluorescence was found in hematopoietic cells in the caudal hematopoietic tissue, thymus, and kidney, but not in parenchymal GFP^+ primitive MG (Figure S6). In contrast, confocal microscopy analyses of brain sections from adult transgenic fish revealed robust labeling of MG, with 36.1% ± 10.9% GFP^+ cells expressing DsRed (Figures 6B and 6C). In comparison, no *DsRed*$^+$ cells were found in control brains from adult Tg(*UAS:Cre*; *ßactin:Switch-DsRed*; *mpeg1:GFP*) (Figure 6C). Importantly, although not all adult MG were marked in these experiments, within individual fish, the proportions of *DsRed*$^+$ MG and *DsRed*$^+$ leukocytes in the WKM, the site of adult hematopoiesis, were highly correlated (Figure 6D), supporting the hypothesis of a common ancestor. Taken together, our data establish embryonic HSCs as a major source of adult MG in the zebrafish.

DISCUSSION

Although several candidates have been suggested, the precise nature of MG progenitors remains a matter of intense debate. This is due, in part, to the lineage-tracing methodologies employed in the murine model that cannot precisely discriminate each subset of hematopoietic precursors. Because each precursor population, namely pMFs, EMPs, and HSCs, arise in distinct anatomical locations at different time points during zebrafish development, we have chosen this vertebrate model to investigate MG ontogeny. Our results demonstrate that the MG network is established through two successive and independent waves of hematopoietic precursors and further identifies the cellular origin of each MG wave. By combining analyses of hematopoietic mutants and cell-specific lineage-tracing approaches, we show here that pMFs generate a first, transient wave that is followed by the establishment of a permanent population originating from embryonic HSCs. Our results uncovering pMFs as the cellular origin of MG are consistent with a previous report that demonstrated, using laser-inducible spatial and temporal restricted activation of Cre, that the rostral blood island (RBI), a region equivalent to the mouse yolk sac and known as the site of pMF production, displays MG potential in the zebrafish embryo (Xu et al., 2015). This study further identified the ventral wall of the dorsal aorta, which includes the hemogenic endothelium that produces HSCs, as the source of a second MG wave that starts to replace rostral blood island-derived MG in the brain parenchyma at around 15 dpf. Taking advantage of the ability of the bloodless *cmyb* mutant to survive through passive oxygen diffusion, Xu and colleagues further showed that MG were present in 3-week-old *cmyb*^{null} juveniles. These observations led the authors to conclude that *cmyb* was not required for adult MG, therefore excluding HSCs as possible progenitors. However, it is likely that most of the MG observed in these experiments were pMF-derived, as our results show that 75% of MG are still of primitive origin at this stage. By taking a different approach (HSC transplantation rescue experiments) allowing us to carry

out phenotypic analyses in adult *cmyb*-deficient animals, we demonstrate here that definitive MG indeed rely upon this master regulator of vertebrate definitive hematopoiesis. Moreover, precise lineage tracing of *gata2b*$^{+}$ embryonic HSCs resulted in labeled adult MG, therefore identifying *cmyb*-dependent embryonic HSCs as the source of definitive MG. Although a possible contribution of other unlabeled progenitors to adult MG ontogeny cannot be excluded from these experiments, the partial labeling of adult MG that we observed in Tg(*gata2b*:Gal4; *UAS:Cre*; *ßactin:Switch-DsRed*) is likely due to inefficient Cre recombination efficiency in *gata2b*$^{+}$ embryonic HSCs, as reflected by the incomplete labeling of the adult WKM blood compartment. Trans-generational silencing of UAS-regulated transgenes through CpG methylation has been reported in zebrafish (Akitake et al., 2011) and might explain the reduction in HSC labeling that we observed in this study. Thus, considering that WKM-derived hematopoiesis originates entirely from embryonic HSCs (Bertrand et al., 2010; Butko et al., 2015), these observations imply that our model likely underestimates the contribution of HSCs in the establishment of the adult MG network. Interestingly, an intriguing question that has emerged from this work is the temporal delay that occurs between HSC specification (completed by 60 hpf) and the emergence of the second MG wave in the CNS (starting at around 20 dpf). Future studies will be necessary to understand whether newly born HSCs directly enter the brain or migrate to an intermediate niche prior to CNS colonization.

A major finding of our study is the demonstration that the zebrafish MG network is established without any contribution from EMPs. Together with previous observations that the PBI, the anatomical site of EMP emergence, lacks both short- and long-term MG potential (Xu et al., 2015), our results now oppose the commonly accepted model of MG development established in the mouse. Over the last few years, many fate-mapping studies have been conducted to investigate the contribution of fetal hematopoiesis to MG ontogeny. Central to these experiments was the use of tamoxifen-inducible Runx1^{MercreMer} and Csf1r^{MercreMer} mice to permanently tag embryonic hematopoietic progenitors and assess the status of MG at later developmental stages. In a study by Ginhoux et al. (2010), genetic labeling of *Runx1*$^{+}$ cells between E7 and E7.5 resulted in 30% of the adult MG pool being marked. By comparison, injection of tamoxifen between E8.5 and E10 did not label adult MG, but efficiently marked circulating monocytes (Ginhoux et al., 2010). In agreement with this time window, additional investigations performed using Csf1r^{MercreMer} mice further indicated that MG arise from *Csf1r*$^{+}$ embryonic cells that can be genetically labeled from E7.5 onward (DeFalco et al., 2014; Epelman et al., 2014; Gomez Perdiguero et al., 2015; Hoeffel et al., 2015; Mossadegh-Keller et al., 2017; Schulz et al., 2012). Collectively, these studies highlighted a developmental relationship between early yolk sac precursors and MG, leading to the consensus that EMPs serve as the source of fetal and perinatal MG. However, yolk sac-derived hematopoiesis is complex and there has been some confusion in the MG field regarding the nature of the different yolk sac-derived myeloid progenitors and the terminology used to define them. One example is the wide assumption that pMFs and EMPs belong to the same lineage, whereas in fact they represent two independent hematopoietic lineages, in respect to their cellular origin, temporal specification, hematopoietic potential, and developmental program (McGrath et al., 2015). Since most fate-mapping studies performed previously in the mouse model did not consider pMFs and EMPs as two distinct populations, the relative MG potential of each yolk sac-derived progenitor cell subset *in vivo* has remained unclear. This is especially important because none of the Cre-ER^{t2} mouse lines used previously to define the source of MG are specific for either pMFs or EMPs, or even HSCs. Indeed, *Runx1* is expressed in and required for the specification of all three lineages (Chen et al., 2009, 2011), and *csf1r* is expressed by all MFs (Sasmono et al., 2003), regardless of their primitive or definitive origin. As the different waves of yolk sac myelopoiesis occur concomitantly during mouse development (between E7.5 and E8.5), a pulse of tamoxifen cannot target a single wave of yolk sac progenitors, and most likely labels pMFs and EMPs simultaneously when injected between E7 and E9. By devising lineage-tracing strategies to discriminate and specifically follow each population, we demonstrate in the zebrafish that pMFs are the sole contributors to embryonic MG. We thus term the initial wave of MG "primitive" to conform to the traditional developmental terminology and to distinguish this first wave from the later "definitive" wave that persists throughout adulthood. Our findings also provide compelling evidence that the establishment of murine embryonic MG relies on the presence of functional pMFs, thus highlighting conservation between species. In a recent report, Hoeffel et al. (2015) proposed to categorize the mouse EMP population into early c-*Myb*-independent EMPs and late *c-Myb*-dependent EMPs, emerging in the yolk sac at E7.5 and E8.25, respectively. Through pulse labeling of *Csf1r*$^{+}$ cells at E8.5, supposed to differentially mark both populations, they suggested that the MG potential was exclusively contained within the c-Myb^{-} EMP subset, while other tissue-resident MFs in the liver, skin, and lung mainly originated from c-Myb^{+} EMPs. Considering the phenotypic and functional similarities between the early c-Myb^{-} EMP population and pMFs (anatomical site and timing of emergence, *c-Myb* dispensability, and lack of erythroid potential), it is likely that the labeling attributed to c-Myb^{-} EMPs was due to labeling of pMFs, which were not considered in this report. If so, the data obtained from this study may support a unique contribution of pMFs to murine embryonic MG, as we describe in the zebrafish.

Our study also highlights possible evolutionary differences regarding the ontogeny of adult MG in vertebrates. Indeed, the complete replacement of embryonic MG by an adult population appears to be specific to zebrafish, as fate-mapping studies performed in the mouse demonstrated adult input from yolk sac-derived hematopoietic progenitors. Interestingly, however, a series of recent observations may provide support for the existence of multiple sources of MG progenitors that arise independently of the yolk sac during murine development. One piece of evidence comes from *in vivo* cell ablation studies in which depletion of yolk sac MFs was obtained through transient pharmacological blocking of CSF1R signaling (Hoeffel et al., 2015; Squarzoni et al., 2014). As expected, ablation of early embryonic MFs resulted in the absence of MG at E14.5. Surprisingly, postnatal MG were not affected by this treatment, as their number was normal from post-natal day 7 (P7) onward (Hoeffel et al., 2015;

Squarzoni et al., 2014). The source of the repopulating postnatal MG in this setting is currently unknown. Also, it was previously reported that adult MG include a subpopulation of *Hoxb8*-expressing cells that infiltrate the brain parenchyma after birth (Chen et al., 2010). Interestingly, besides the *Hoxb8*$^{+}$ MG subset, the lineage tracing of *Hoxb8*$^{+}$ cells labeled most of the hematopoietic compartment in the bone marrow and peripheral blood, suggesting a common HSC origin (Chen et al., 2010). However, further research will be required to address the cellular origin of the *Hoxb8*$^{+}$ MG subset since several reports in the mouse concluded that genetic labeling of conventional embryonic HSCs did not result in a switch of adult MG. Nevertheless, these findings in the mouse model raise the possibility of MG progenitors migrating in the postnatal brain in physiological conditions, as we observe in the zebrafish. Understanding the mechanisms underlying the emergence of these cells in the CNS, possibly after the sealing of the blood-brain barrier, may thus have profound biological and therapeutic implications.

In conclusion, our study provides insights into the ontogeny of MG by unambiguously demonstrating that pMFs serve as the unique source of primitive MG in the zebrafish embryo. Taken together, our findings also indicate that different precursors generate embryonic and adult MG in the zebrafish, and suggest that the cellular and molecular mechanisms underlying MG ontogeny in mammals may be more complex than previously thought, as recently shown for other populations of tissue-resident MFs (Molawi et al., 2014; Mossadegh-Keller et al., 2017). Given the multiple roles of MG in CNS development, homeostasis, and disease, it will be of great interest to determine whether these different developmental pathways confer differential functions to each MG subset.

EXPERIMENTAL PROCEDURES

Zebrafish

Zebrafish were maintained under standard conditions and in accordance with institutional (Université Libre de Bruxelles [ULB]) and national ethical and animal welfare guidelines and regulation. All experimental procedures are approved by the ethical committee for animal welfare (CEBEA) from the ULB (protocol 594N). The following lines were used: AB*, *Tg(mhc2dab:GFP-LT)*^{sd6} (Wittamer et al., 2011), *Tg(ptprc:DsRed*^{express}*)*^{sd3} (Wittamer et al., 2011), *Tg(mpeg1:eGFP)*^{gl22} (Ellett et al., 2011), *Tg(−6.0itga2b*:eGFP*)*^{la} (Lin et al., 2005), *Tg(kdrl:Cre)*^{s898} (Bertrand et al., 2010), *Tg(actb2:loxP-STOP-loxP-DsRed*^{express}*)*^{sd5} (Bertrand et al., 2010), *Tg(mpeg1:Gal4)*^{gl24} (Ellett et al., 2011), *Tg(UAS-E1b:Kaede)*^{s1999t} (Ellett et al., 2011), *cmyb*^{t25127} (Soza-Ried et al., 2010), *laf*^{fm110b} (Hogan et al., 2006), *tfec*^{ug103} (Mahony et al., 2016), *TgBAC(gata2b:KalTA4)*^{sd32} (Butko et al., 2015), and *Tg(UAS:Cre,CY)*^{zd17} (Butko et al., 2015). For clarity, throughout the text, transgenic animals are referred to without allele designations: *TgBAC(gata2b:KalTA4)*^{sd32} is referred to as *Tg(gata2b:Gal4)*; *Tg(UAS:Cre,CY)*^{zd17} is referred to as *Tg(UAS:Cre)*; and *ptprc* and *itga2b* are referred to as *cd45* and *cd41*, respectively.

Whole-Mount RNA *In Situ* Hybridization

Antisense DIG-labeled *mfap4*, *rag1*, and *apoeb* RNA probes were synthesized *in vitro*. Zebrafish embryos at the desired stages were fixed in 4% paraformaldehyde (PFA). Whole-mount RNA *in situ* hybridization (WISH) was performed using standard methods (Thisse and Thisse, 2008).

Fluorescent Microscopy

Embryos and larvae (up to 10 dpf) were fixed in 4% PFA, and then directly subjected to whole-mount antibody staining. For juvenile and adult fish, the brains were dissected, fixed in 4% PFA, and subjected to either tissue clearing and imaging (15- to 50-dpf fish), or incubated overnight in 30% sucrose and applied to cryosection followed by antibody staining (adult fish). The following antibodies were used: chicken anti-GFP polyclonal antibody (1:1,000; Abcam), rabbit anti-DsRed polyclonal antibody (1:1,000; Clontech), Alexa Fluor 488-conjugated anti-chicken IgG antibody (1:500; Invitrogen), and Alexa Fluor 594-conjugated anti-rabbit IgG (1:500; Abcam). Images were taken with a Zeiss LSM 780 inverted microscope, using the following objectives: EC Plan Neofluar 10×, Plan Apochromat 20×, LD LCI Plan Apochromat 25×, and LD C Apochromat 40×.

Statistical Analyses

Statistical analyses were performed with the GraphPad Prism software, using an unpaired Student t test. Each dot plot value represents an independent embryo, and every experiment was conducted three times independently.

SUPPLEMENTAL INFORMATION

Supplemental Information includes Supplemental Experimental Procedures, six figures, and one table and can be found with this article online at https://doi.org/10.1016/j.celrep.2018.05.066.

ACKNOWLEDGMENTS

We thank J.-M. Vanderwinden and the LiMiF for technical support with confocal imaging, Christine Dubois for help with flow cytometry, Chantal Combepine and Naoual Azeroual for technical assistance, and Karen Ong for laboratory maintenance (D.T. lab). V.W. is an investigator of WELBIO and is also supported by grants from the Fonds National de la Recherche Scientifique (FNRS), Innoviris (BB2B Programme), and The Minerve Foundation. J.Y.B. is endorsed by a Chair in Life Sciences funded by the Gabriella Giorgi-Cavaglieri Foundation and is also funded by the Swiss National Fund (31003_166515). D.T. is supported by R21 AI124179 from the National Institutes of Health and C.R. by a European Research Council grant (ERC Project Number 220-H75001EU/HSCOrigin-309361), a TOP subsidy from NWO/ZonMw (912.15.017), and the UMC Utrecht "Regenerative Medicine & Stem Cells" Priority Research Program. G.F. received funding from UNI and FNRS fellowships, and E.D.R. received funding from a FRIA fellowship.

AUTHOR CONTRIBUTIONS

D.T., J.Y.B., and V.W. designed the research and directed the study. G.F., C.B.M., E.D., E.D.R., M.M., M.C., J.Y.B., and V.W. performed zebrafish experiments. L.Y. and C.R. performed mouse experiments. Initial studies were performed in D.T.'s laboratory. J.Y.B. and V.W. wrote the manuscript with comments from all authors.

DECLARATION OF INTERESTS

The authors declare no competing interests.

Received: November 28, 2017
Revised: April 17, 2018
Accepted: May 18, 2018
Published: July 3, 2018

REFERENCES

Ajami, B., Bennett, J.L., Krieger, C., Tetzlaff, W., and Rossi, F.M. (2007). Local self-renewal can sustain CNS microglia maintenance and function throughout adult life. Nat. Neurosci. *10*, 1538–1543.

Akitake, C.M., Macurak, M., Halpern, M.E., and Goll, M.G. (2011). Transgenerational analysis of transcriptional silencing in zebrafish. Dev. Biol. *352*, 191–201.

Alliot, F., Godin, I., and Pessac, B. (1999). Microglia derive from progenitors, originating from the yolk sac, and which proliferate in the brain. Brain Res. Dev. Brain Res. *117*, 145–152.

Bertrand, J.Y., Jalil, A., Klaine, M., Jung, S., Cumano, A., and Godin, I. (2005). Three pathways to mature macrophages in the early mouse yolk sac. Blood *106*, 3004–3011.

Bertrand, J.Y., Kim, A.D., Violette, E.P., Stachura, D.L., Cisson, J.L., and Traver, D. (2007). Definitive hematopoiesis initiates through a committed erythromyeloid progenitor in the zebrafish embryo. Development *134*, 4147–4156.

Bertrand, J.Y., Chi, N.C., Santoso, B., Teng, S., Stainier, D.Y., and Traver, D. (2010). Haematopoietic stem cells derive directly from aortic endothelium during development. Nature *464*, 108–111.

Boche, D., Perry, V.H., and Nicoll, J.A. (2013). Review: activation patterns of microglia and their identification in the human brain. Neuropathol. Appl. Neurobiol. *39*, 3–18.

Butko, E., Distel, M., Pouget, C., Weijts, B., Kobayashi, I., Ng, K., Mosimann, C., Poulain, F.E., McPherson, A., Ni, C.W., et al. (2015). Gata2b is a restricted early regulator of hemogenic endothelium in the zebrafish embryo. Development *142*, 1050–1061.

Butovsky, O., Jedrychowski, M.P., Moore, C.S., Cialic, R., Lanser, A.J., Gabriely, G., Koeglsperger, T., Dake, B., Wu, P.M., Doykan, C.E., et al. (2014). Identification of a unique TGF-β-dependent molecular and functional signature in microglia. Nat. Neurosci. *17*, 131–143.

Chen, M.J., Yokomizo, T., Zeigler, B.M., Dzierzak, E., and Speck, N.A. (2009). Runx1 is required for the endothelial to haematopoietic cell transition but not thereafter. Nature *457*, 887–891.

Chen, S.K., Tvrdik, P., Peden, E., Cho, S., Wu, S., Spangrude, G., and Capecchi, M.R. (2010). Hematopoietic origin of pathological grooming in Hoxb8 mutant mice. Cell *141*, 775–785.

Chen, M.J., Li, Y., De Obaldia, M.E., Yang, Q., Yzaguirre, A.D., Yamada-Inagawa, T., Vink, C.S., Bhandoola, A., Dzierzak, E., and Speck, N.A. (2011). Erythroid/myeloid progenitors and hematopoietic stem cells originate from distinct populations of endothelial cells. Cell Stem Cell *9*, 541–552.

Colonna, M., and Butovsky, O. (2017). Microglia function in the central nervous system during health and neurodegeneration. Annu. Rev. Immunol. *35*, 441–468.

Cuadros, M.A., Martin, C., Coltey, P., Almendros, A., and Navascués, J. (1993). First appearance, distribution, and origin of macrophages in the early development of the avian central nervous system. J. Comp. Neurol. *330*, 113–129.

Davalos, D., Grutzendler, J., Yang, G., Kim, J.V., Zuo, Y., Jung, S., Littman, D.R., Dustin, M.L., and Gan, W.B. (2005). ATP mediates rapid microglial response to local brain injury in vivo. Nat. Neurosci. *8*, 752–758.

DeFalco, T., Bhattacharya, I., Williams, A.V., Sams, D.M., and Capel, B. (2014). Yolk-sac-derived macrophages regulate fetal testis vascularization and morphogenesis. Proc. Natl. Acad. Sci. USA *111*, E2384–E2393.

Ellett, F., Pase, L., Hayman, J.W., Andrianopoulos, A., and Lieschke, G.J. (2011). mpeg1 promoter transgenes direct macrophage-lineage expression in zebrafish. Blood *117*, e49–e56.

Epelman, S., Lavine, K.J., Beaudin, A.E., Sojka, D.K., Carrero, J.A., Calderon, B., Brija, T., Gautier, E.L., Ivanov, S., Satpathy, A.T., et al. (2014). Embryonic and adult-derived resident cardiac macrophages are maintained through distinct mechanisms at steady state and during inflammation. Immunity *40*, 91–104.

Frame, J.M., McGrath, K.E., and Palis, J. (2013). Erythro-myeloid progenitors: "definitive" hematopoiesis in the conceptus prior to the emergence of hematopoietic stem cells. Blood Cells Mol. Dis. *51*, 220–225.

Frame, J.M., Fegan, K.H., Conway, S.J., McGrath, K.E., and Palis, J. (2016). Definitive hematopoiesis in the yolk sac emerges from Wnt-responsive hemogenic endothelium independently of circulation and arterial identity. Stem Cells *34*, 431–444.

Ginhoux, F., Greter, M., Leboeuf, M., Nandi, S., See, P., Gokhan, S., Mehler, M.F., Conway, S.J., Ng, L.G., Stanley, E.R., et al. (2010). Fate mapping analysis reveals that adult microglia derive from primitive macrophages. Science *330*, 841–845.

Gomez Perdiguero, E., Klapproth, K., Schulz, C., Busch, K., Azzoni, E., Crozet, L., Garner, H., Trouillet, C., de Bruijn, M.F., Geissmann, F., and Rodewald, H.R. (2015). Tissue-resident macrophages originate from yolk-sac-derived erythro-myeloid progenitors. Nature *518*, 547–551.

Guerreiro, R., Wojtas, A., Bras, J., Carrasquillo, M., Rogaeva, E., Majounie, E., Cruchaga, C., Sassi, C., Kauwe, J.S., Younkin, S., et al.; Alzheimer Genetic Analysis Group (2013). TREM2 variants in Alzheimer's disease. N. Engl. J. Med. *368*, 117–127.

Herbomel, P., Thisse, B., and Thisse, C. (1999). Ontogeny and behaviour of early macrophages in the zebrafish embryo. Development *126*, 3735–3745.

Herbomel, P., Thisse, B., and Thisse, C. (2001). Zebrafish early macrophages colonize cephalic mesenchyme and developing brain, retina, and epidermis through a M-CSF receptor-dependent invasive process. Dev. Biol. *238*, 274–288.

Hess, I., Iwanami, N., Schorpp, M., and Boehm, T. (2013). Zebrafish model for allogeneic hematopoietic cell transplantation not requiring preconditioning. Proc. Natl. Acad. Sci. USA *110*, 4327–4332.

Hoeffel, G., Chen, J., Lavin, Y., Low, D., Almeida, F.F., See, P., Beaudin, A.E., Lum, J., Low, I., Forsberg, E.C., et al. (2015). C-Myb^{+} erythro-myeloid progenitor-derived fetal monocytes give rise to adult tissue-resident macrophages. Immunity *42*, 665–678.

Hogan, B.M., Layton, J.E., Pyati, U.J., Nutt, S.L., Hayman, J.W., Varma, S., Heath, J.K., Kimelman, D., and Lieschke, G.J. (2006). Specification of the primitive myeloid precursor pool requires signaling through Alk8 in zebrafish. Curr. Biol. *16*, 506–511.

Kierdorf, K., Erny, D., Goldmann, T., Sander, V., Schulz, C., Perdiguero, E.G., Wieghofer, P., Heinrich, A., Riemke, P., Hölscher, C., et al. (2013). Microglia emerge from erythromyeloid precursors via Pu.1- and Irf8-dependent pathways. Nat. Neurosci. *16*, 273–280.

Kissa, K., and Herbomel, P. (2010). Blood stem cells emerge from aortic endothelium by a novel type of cell transition. Nature *464*, 112–115.

Li, Y., Du, X.F., Liu, C.S., Wen, Z.L., and Du, J.L. (2012). Reciprocal regulation between resting microglial dynamics and neuronal activity in vivo. Dev. Cell *23*, 1189–1202.

Lin, H.F., Traver, D., Zhu, H., Dooley, K., Paw, B.H., Zon, L.I., and Handin, R.I. (2005). Analysis of thrombocyte development in CD41-GFP transgenic zebrafish. Blood *106*, 3803–3810.

Mahony, C.B., Fish, R.J., Pasche, C., and Bertrand, J.Y. (2016). tfec controls the hematopoietic stem cell vascular niche during zebrafish embryogenesis. Blood *128*, 1336–1345.

Mass, E., Jacome-Galarza, C.E., Blank, T., Lazarov, T., Durham, B.H., Ozkaya, N., Pastore, A., Schwabenland, M., Chung, Y.R., Rosenblum, M.K., et al. (2017). A somatic mutation in erythro-myeloid progenitors causes neurodegenerative disease. Nature *549*, 389–393.

McGrath, K.E., Frame, J.M., and Palis, J. (2015). Early hematopoiesis and macrophage development. Semin. Immunol. *27*, 379–387.

Medvinsky, A., Rybtsov, S., and Taoudi, S. (2011). Embryonic origin of the adult hematopoietic system: advances and questions. Development *138*, 1017–1031.

Mildner, A., Schmidt, H., Nitsche, M., Merkler, D., Hanisch, U.K., Mack, M., Heikenwalder, M., Brück, W., Priller, J., and Prinz, M. (2007). Microglia in the adult brain arise from Ly-6ChiCCR2^{+} monocytes only under defined host conditions. Nat. Neurosci. *10*, 1544–1553.

Molawi, K., Wolf, Y., Kandalla, P.K., Favret, J., Hagemeyer, N., Frenzel, K., Pinto, A.R., Klapproth, K., Henri, S., Malissen, B., et al. (2014). Progressive replacement of embryo-derived cardiac macrophages with age. J. Exp. Med. *211*, 2151–2158.

Mossadegh-Keller, N., Gentek, R., Gimenez, G., Bigot, S., Mailfert, S., and Sieweke, M.H. (2017). Developmental origin and maintenance of distinct testicular macrophage populations. J. Exp. Med. *214*, 2829–2841.

Nimmerjahn, A., Kirchhoff, F., and Helmchen, F. (2005). Resting microglial cells are highly dynamic surveillants of brain parenchyma in vivo. Science *308*, 1314–1318.

Paloneva, J., Manninen, T., Christman, G., Hovanes, K., Mandelin, J., Adolfsson, R., Bianchin, M., Bird, T., Miranda, R., Salmaggi, A., et al. (2002).

Mutations in two genes encoding different subunits of a receptor signaling complex result in an identical disease phenotype. Am. J. Hum. Genet. *71*, 656–662.

Peri, F., and Nüsslein-Volhard, C. (2008). Live imaging of neuronal degradation by microglia reveals a role for v0-ATPase a1 in phagosomal fusion in vivo. Cell *133*, 916–927.

Prinz, M., Erny, D., and Hagemeyer, N. (2017). Ontogeny and homeostasis of CNS myeloid cells. Nat. Immunol. *18*, 385–392.

Rademakers, R., Baker, M., Nicholson, A.M., Rutherford, N.J., Finch, N., Soto-Ortolaza, A., Lash, J., Wider, C., Wojtas, A., DeJesus-Hernandez, M., et al. (2011). Mutations in the colony stimulating factor 1 receptor (CSF1R) gene cause hereditary diffuse leukoencephalopathy with spheroids. Nat. Genet. *44*, 200–205.

Ransohoff, R.M., and Cardona, A.E. (2010). The myeloid cells of the central nervous system parenchyma. Nature *468*, 253–262.

Sasmono, R.T., Oceandy, D., Pollard, J.W., Tong, W., Pavli, P., Wainwright, B.J., Ostrowski, M.C., Himes, S.R., and Hume, D.A. (2003). A macrophage colony-stimulating factor receptor-green fluorescent protein transgene is expressed throughout the mononuclear phagocyte system of the mouse. Blood *101*, 1155–1163.

Schmid, C.D., Melchior, B., Masek, K., Puntambekar, S.S., Danielson, P.E., Lo, D.D., Sutcliffe, J.G., and Carson, M.J. (2009). Differential gene expression in LPS/IFNgamma activated microglia and macrophages: in vitro versus in vivo. J. Neurochem. *109* (*Suppl 1*), 117–125.

Schulz, C., Gomez Perdiguero, E., Chorro, L., Szabo-Rogers, H., Cagnard, N., Kierdorf, K., Prinz, M., Wu, B., Jacobsen, S.E., Pollard, J.W., et al. (2012). A lineage of myeloid cells independent of Myb and hematopoietic stem cells. Science *336*, 86–90.

Sieger, D., Moritz, C., Ziegenhals, T., Prykhozhij, S., and Peri, F. (2012). Long-range Ca^{2+} waves transmit brain-damage signals to microglia. Dev. Cell *22*, 1138–1148.

Soza-Ried, C., Hess, I., Netuschil, N., Schorpp, M., and Boehm, T. (2010). Essential role of c-*myb* in definitive hematopoiesis is evolutionarily conserved. Proc. Natl. Acad. Sci. USA *107*, 17304–17308.

Squarzoni, P., Oller, G., Hoeffel, G., Pont-Lezica, L., Rostaing, P., Low, D., Bessis, A., Ginhoux, F., and Garel, S. (2014). Microglia modulate wiring of the embryonic forebrain. Cell Rep. *8*, 1271–1279.

Sumner, R., Crawford, A., Mucenski, M., and Frampton, J. (2000). Initiation of adult myelopoiesis can occur in the absence of c-Myb whereas subsequent development is strictly dependent on the transcription factor. Oncogene *19*, 3335–3342.

Thisse, C., and Thisse, B. (2008). High-resolution in situ hybridization to whole-mount zebrafish embryos. Nat. Protoc. *3*, 59–69.

Traver, D., Paw, B.H., Poss, K.D., Penberthy, W.T., Lin, S., and Zon, L.I. (2003). Transplantation and in vivo imaging of multilineage engraftment in zebrafish bloodless mutants. Nat. Immunol. *4*, 1238–1246.

Wittamer, V., Bertrand, J.Y., Gutschow, P.W., and Traver, D. (2011). Characterization of the mononuclear phagocyte system in zebrafish. Blood *117*, 7126–7135.

Wolf, S.A., Boddeke, H.W., and Kettenmann, H. (2017). Microglia in physiology and disease. Annu. Rev. Physiol. *79*, 619–643.

Xu, J., Zhu, L., He, S., Wu, Y., Jin, W., Yu, T., Qu, J.Y., and Wen, Z. (2015). Temporal-spatial resolution fate mapping reveals distinct origins for embryonic and adult microglia in zebrafish. Dev. Cell *34*, 632–641.

Xu, J., Wang, T., Wu, Y., Jin, W., and Wen, Z. (2016). Microglia colonization of developing zebrafish midbrain is promoted by apoptotic neuron and lysophosphatidylcholine. Dev. Cell *38*, 214–222.